

This is a self-archived version of an original article. This version may differ from the original in pagination and typographic details.

Author(s): Tirronen, Maria; Hutchings, Jeffrey A.; Pardo, Sebastián A.; Kuparinen, Anna

Title: Atlantic salmon survival at sea : temporal changes that lack regional synchrony

Year: 2022

Version: Accepted version (Final draft)

Copyright: © 2022 The Author(s).


Rights: CC BY 4.0

Rights url: https://creativecommons.org/licenses/by/4.0/deed.en_GB

Please cite the original version:

Tirronen, M., Hutchings, J. A., Pardo, S. A., & Kuparinen, A. (2022). Atlantic salmon survival at sea : temporal changes that lack regional synchrony. *Canadian Journal of Fisheries and Aquatic Sciences*, 79(10), 1697-1711. <https://doi.org/10.1139/cjfas-2021-0302>

Atlantic salmon survival at sea: temporal changes that lack regional synchrony

Maria Tirronen ^a, Jeffrey A. Hutchings^{b,c,d}, Sebastián A. Pardo^{b,e}, and Anna Kuparinen^a

^aDepartment of Biological and Environmental Science, University of Jyväskylä, FI-40014, Jyväskylä, Finland; ^bDepartment of Biology, Dalhousie University, Halifax, NS B3H 4R2, Canada; ^cInstitute of Marine Research, Flødevigen Marine Research Station, His, N-4817, Norway; ^dDepartment of Natural Sciences, University of Agder, Kristiansand, N-4604, Norway; ^eEcology Action Centre, Halifax, NS B3K 4L3, Canada

Corresponding author: Maria Tirronen (email: maria.j.e.tirronen@jyu.fi)

Abstract

Spatial and temporal synchrony in abundance or survival trends can be indicative of whether populations are affected by common environmental drivers. In Atlantic salmon (*Salmo salar*), return rates to natal rivers have generally been assumed to be affected primarily by shared oceanic conditions, leading to spatially synchronous trends in mortality. Here, we investigated the existence of parallel trends in salmon sea survival, using data on migrating smolts and returning adults from seven Canadian populations presumed to share feeding grounds. We analysed sea survival, using a Bayesian change-point model capable of detecting nonstationarity in time series data. Our results indicate that while salmon have experienced broadly comparable patterns in survival, finer-scale temporal shifts are not synchronous among populations. Our findings are not consistent with the hypothesis that salmon populations consistently share the same mortality-related stressors in the marine environment. Although populations may have shared greater synchrony in survival patterns in the past, this synchrony may be breaking down. It may be prudent to direct greater attention to smaller-scale regional and population-level correlates of survival.

Résumé

Le synchronisme spatial et temporel des tendances d'abondance ou de survie peut indiquer si différentes populations sont influencées par les mêmes facteurs environnementaux. Il est généralement présumé que, chez les saumons atlantiques (*Salmo salar*), les taux de retour aux rivières natales sont principalement influencés par des conditions océaniques communes, ce qui mène à des tendances de mortalité synchrones dans l'espace. Nous examinons l'existence de tendances parallèles de survie en mer des saumons en utilisant des données sur les saumoneaux migrants et les adultes retournant dans leur rivière natale de sept populations canadiennes présumées avoir les mêmes aires d'alimentation. Nous analysons la survie en mer en utilisant un modèle bayésien de points de changement pouvant détecter la présence de non-stationnarité dans les données de séries chronologiques. Nos résultats indiquent que, bien que les saumons présentent des motifs de survie généralement semblables, des changements temporels à échelle plus fine ne sont pas synchrones d'une population à l'autre. Nos résultats ne concordant pas avec l'hypothèse voulant que les populations de saumons aient toujours en commun les mêmes facteurs de stress reliés à la mortalité dans le milieu marin. Si les motifs de survie des populations peuvent avoir présenté un plus grand synchronisme par le passé, ce synchronisme pourrait être en train de s'effriter. Il peut être prudent d'accorder plus d'attention aux corrélats de la survie à des échelles régionales ou populationnelles plus fines. [Traduit par la Rédaction]

1. Introduction

The viability of a species depends on the resistance and resilience of its constituent populations to natural and human-induced environmental change. Reduced viability reflects reductions in the abundance or survival of one or more of these constituent populations. Under such circumstances, and when multiple populations are implicated, attempts to understand and mitigate species' threats lead to two fundamental questions. Firstly, to what extent do the separate populations share similar overall trends in trajectory in abun-

dance or survival? If they are all declining, it would be suggestive of a similarly shared threat. If abundance or survival trajectories differ in overall temporal sign (some increasing, some declining, some remaining stable), it could be inferred that the underlying causes of population change differ, possibly giving rise to a "portfolio effect" that can underpin the viability of some species (Schindler et al. 2010). For those sharing similar overall patterns of population decline, a second but related question is whether the beginning of the decline, and subsequent intermittent temporal changes in trajectory,

occur simultaneously among populations. The former would be suggestive of a common threat, the latter (depending on time lags) suggestive of different threats.

Among vertebrates, particularly those of perceived exploitative or charismatic value, there are often sufficient data to monitor changes in at least one population for many species (e.g., livingplanetindex.org). For some species, the data are comparatively rich, albeit highly variable in quality and temporal resolution. One of these is Atlantic salmon (*Salmo salar*). The highest number of wild populations are found in Norway and in Canada (ICES 2021). Catch statistics of salmon stocks in Norway peaked in the 1960s and 1970s and since then, catches have diminished (WWF 2001). Compared to the estimated abundance of wild Norwegian salmon (including those caught by fishing) in the mid-1980s, numbers were reduced by about half thereafter, and have been fairly stable since the early 1990s, excepting a short-term peak at the turn of the 21st century (SCSM 2019). A remarkably similar pattern in overall pre-fishery abundance is evident for wild Canadian salmon (for which the earliest time series extend to the 1970s): high abundance until the mid-1980s followed by decline until the early 1990s and relative stability since (ICES 2021).

Reasons for the initial abundance declines and subsequent lack of recovery have been attributed to numerous additive and interactive influences. For example, among the current stressors identified for wild Norwegian salmon, the top five include farmed escapees and pathogens originating from salmon aquaculture, freshwater habitat alteration (e.g., barriers to migration), acidification, and hydroelectric development (SCSM 2019). Several studies provide support for the hypothesis that the initial decline of salmon in the late 1980s and early 1990s was precipitated by increased mortality in the marine environment (e.g., Massiot-Granier et al. 2014).

Questions related to the causes of this increased salmon mortality can be addressed examining patterns of spatial and temporal coherence in population trajectories for survival. Olmos et al. (2019, 2020) reported a strong spatial coherence in temporal survival patterns among 13 “stock units” distributed in North America and southern Europe. Their findings suggest that factors affecting salmon mortality at sea are temporally consistent at broad (North Atlantic) and smaller (stock unit) spatial scales.

One key data challenge when studying Atlantic salmon mortality, and its potential spatial and temporal coherence among populations, is the near absence of empirical abundance information on salmon prior to and during their migration to the ocean (Olmos et al. 2019; ICES 2021). Perhaps the most important developmental stage in this respect is the smolt stage (the term “smolt” describes salmon during their downstream migration to the ocean; the term “post-smolt” typically encompasses the first 3–6 months of a salmon’s life at sea). For example, of the 199 populations (stocks) of salmon for which spawning targets are evaluated in Norway, long-term data on smolts are available for two rivers, only one of which has been monitored since 2010 (SCSM 2019).

The variable quality of data at the population level has led to a tendency to amalgamate population-specific data into stock units, some of which contain tens of populations, oth-

ers hundreds (e.g., ICES 2017; Olmos et al. 2019, 2020). This regional pooling of salmon data, particularly when the identities of the specific constituent populations are not readily identifiable, can present challenges when trying to understand broad- and smaller-scale patterns in survival at the population level. A second issue associated with data amalgamation can be the inclusion of populations that are sustained by hatcheries into the regional or stock units, hatcheries having rather well-documented, often unhelpful influences when evaluating patterns of population survival (Fraser 2008; NASCO 2017).

These challenges suggest utility in undertaking detailed temporal analyses of salmon survival for which the supporting population data are as empirically strong as the best available information allows. There are seven Canadian populations for which detailed information on the number of outmigrating smolts and the number of returning adults exist. These populations are widely distributed throughout the species’ Canadian range, extending from Newfoundland in the north to Nova Scotia in the south. For each of these populations, Pardo et al. (2021) estimated survival of salmon at sea, using a hierarchical Bayesian model that incorporated Murphy’s (1952) maturity schedule model in conjunction with informative priors.

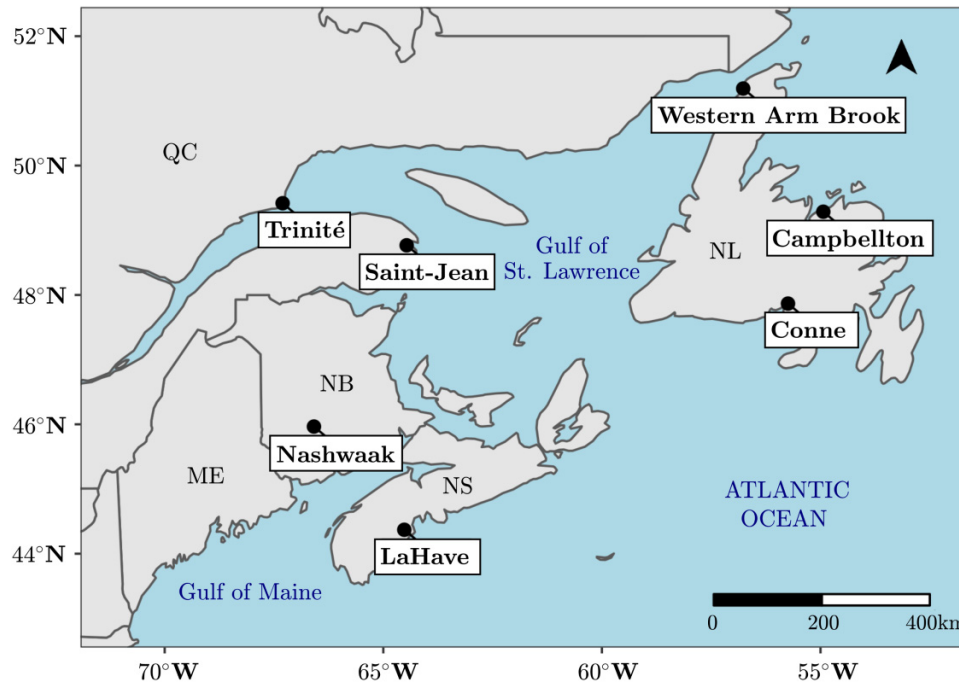
Here, we extended previous work (Olmos et al. 2019; Pardo et al. 2021) and examined whether population patterns in salmon marine survival are concordant or divergent at fine temporal scales of resolution. Our approach involves application of the Bayesian online change-point detection (BOCPD) method developed by Adams and MacKay (2007), combined with simulation-based filtering (Liu and West 2001; Perälä et al. 2017). This method, used previously to analyse temporal changes in stock-recruitment parameters (Perälä et al. 2017; Tirronen et al. 2021) and Atlantic cod (*Gadus morhua*) abundance (Perälä et al. 2020), offers a procedure to detect shifts in the parameters of the data-generating process. We find that temporal shifts in survival at sea may not occur synchronously nor be similar for populations in different rivers.

2. Materials and methods

2.1. Data

We analysed the time series of smolts and returning fish of Atlantic salmon populations in seven rivers in eastern Canada. These populations included Western Arm Brook (WAB; Fig. 1) and the Campbellton and Conne rivers in Newfoundland and Labrador (NL), Rivière de la Trinité and Rivière de la Saint-Jean in Quebec (QC), LaHave River in Nova Scotia’s (NS) Southern Uplands, and Nashwaak River in New Brunswick (NB). The numbers of emigrating smolts were based on two methods. For Trinité, Saint-Jean, LaHave, Nashwaak, and Conne, smolt numbers were estimated from mark-recapture studies. For the WAB and Campbellton populations, smolt numbers were directly recorded at counting fences during their seaward migration. The methods are fully cited by Pardo et al. (2021). The number of returning adults was based on direct counts of small (<63 cm) and large (≥63 cm) salmon. Age determination from scales was done

Fig. 1. Locations of the seven rivers in eastern Canada with temporal data of outmigrating smolts and returning adult Atlantic salmon (adapted from the study by Pardo et al. 2021). The map uses a lat/long (geographic) projection and a WGS 84 datum.



for a subset of returns each year, which allowed for calculating the proportion of different age classes within the size groups, and subsequently estimate the total proportion of each age class among the returning fish (Pardo et al. 2021).

Naturally, the true smolt abundances differ from the observed smolt abundances. Pardo et al. (2021) used a hierarchical Bayesian model to estimate the true abundances. To decrease bias in our results caused by measurement errors, we fitted our model using the medians of the posterior distributions of the true smolt abundances obtained by Pardo et al. (2021) as smolt abundance data. Similarly, the observed returning fish abundances are likely to differ from the true numbers of returning fish. Pardo et al. (2021) estimated these differences, the measurement errors, by bootstrapping. To consider the measurement errors in returning fish abundance data in our model, we utilized the estimates by Pardo et al. (2021).

For three rivers (LaHave, Saint-Jean, and Trinité), there was one or two missing years within their time series. For those years, there had been no smolt count due to too much water flow. In addition, in some years for one-sea-winter (1SW)-dominated populations, estimates of returning two-sea-winter (2SW) fish were zero. These counts were included in the analysis by adding a small quantity to enable log-transformation. Given that the zero counts appeared only in 1SW-dominated populations, small differences in the value of log 2SW returns are not likely to have a considerable impact on the marine survival estimates in the first year at sea.

2.2. Bayesian change-point model

We modelled marine survival of salmon by a Bayesian change-point model that consists of the Murphy's maturity

schedule model combined with an a priori unknown number of change points at which the model parameters, describing survival and years at sea, shift. Marine survival of cohorts in different rivers were modelled separately. For years $t = 1, \dots, T$, where T is the length of the time series, the model relates the observed number of returning 1SW and 2SW fish, $\mathbf{R}_t = (R_t^{1SW}, R_t^{2SW})$, in a given river, to the estimated number of smolts in that river (the posterior medians of the estimated true smolt abundances; Pardo et al. 2021), S_t . For ease of notation, we here use the same subscript for all abundance estimates corresponding to the 1SW fish count at year t , although the smolt and 2SW fish counts were recorded at years $t - 1$ and $t + 1$, respectively. Moreover, the change points divide the data into I regimes, or segments, $\rho = 1, 2, \dots, I$. Given the position of a change point, the data before the change point were assumed to be independent of the data after the change point.

The same underlying predictive model that relates \mathbf{R}_t to S_t was assumed for the data in different segments so that only the values of the model parameters vary between segments. The model parameters of different segments, η_ρ , $\rho = 1, 2, \dots, I$, were assumed to be independent and identically distributed. To estimate the parameter values, we applied the BOCPD method, which processes data in a sequential manner, updating estimates for the parameter values and computing posterior probabilities for a change point after each data item. The approximation of η_ρ at time t , inferred from a current run length r_t , the time elapsed since the last change point, is denoted by $\eta_t^{(r)}$. Moreover, given segmentation and the corresponding parameter values, we assumed that the abundances of different cohorts are mutually independent. Such a simplifying assumption was also made by Pardo et al. (2021).

The Bayesian change-point model consists of the following probability distributions:

$$(1) \quad p(\mathbf{R}_t | S_t, \eta_t^{(r)}), \quad t = 1, \dots, T$$

$$(2) \quad p(\eta_t^{(0)})$$

$$(3) \quad p(r_t | r_{t-1}), \quad t = 2, \dots, T$$

and

$$(4) \quad p(r_1)$$

The output distribution (eq. 1) is defined by the underlying predictive model and (eq. 2) is the joint prior distribution of the model parameters. The transition probability (eq. 3) is the change-point prior, which assumes that the run lengths $r_t \in \{0, 1, \dots, t - 1\}$ form a Markov chain, and (eq. 4) defines the initial run length distribution.

2.3. Underlying predictive model

The average relationship between smolts and 1SW and 2SW fish was represented by the **Murphy's (1952)** maturity schedule model.

$$(5) \quad \widehat{R}^{1SW}(S) = S \cdot s^{1SW} \cdot p$$

$$(6) \quad \widehat{R}^{2SW}(S) = S \cdot s^{1SW} \cdot (1 - p) \cdot s^{2SW}$$

where we omit t and (r) for ease of notation. Above, $s^{1SW}, s^{2SW} \in [0, 1]$ denote the proportions of salmon surviving in their first or second year at sea, respectively, and $p \in [0, 1]$ is the proportion of salmon that return to spawn after 1 year at sea. The model (eqs. 5 and 6) assumes that salmon do not spend more than 2 years at sea and that there are no repeat spawners. In the populations we studied, age 3+ spawners (3SW+) comprise a very small fraction of first-time spawners (**Pardo et al. 2021**). Nonetheless, accounting for 3SW+ fish would likely result in slightly higher estimates for overall survival at sea.

Following **Pardo et al. (2021)**, we assumed that the number of 1SW and 2SW fish are conditionally independent, given

the number of smolts and approximated model parameters. Such an assumption states that deviations from the predicted number of returning fish by the **Murphy's maturity schedule model** do not correlate between 1SW and 2SW fish. More precisely, the logarithms of R^{1SW}, R^{2SW} were modelled as normally distributed random variables.

$$(7) \quad \log(R^a) \sim N\left(\log[\widehat{R}^a(S)], (\sigma^a)^2 + (\epsilon^a)^2\right) \\ a = 1SW, 2SW$$

where σ^a is the standard deviation of yearly variation of 1SW and 2SW fish from the average relationship between smolts and returning fish in log scale and ϵ^a describes yearly estimation error (**Pardo et al. 2021**) in the (log-transformed) number of 1SW and 2SW fish. With eq. 7, the abundances of 1SW and 2SW fish obey lognormal distributions with medians $\widehat{R}^{1SW}(S)$ and $\widehat{R}^{2SW}(S)$, and coefficients of variation.

$$(8) \quad CV^a = \sqrt{\exp[(\sigma^a)^2 + (\epsilon^a)^2] - 1}, \quad a = 1SW, 2SW$$

Overall, the underlying predictive model has five parameters.

$$(9) \quad \eta = (s^{1SW}, s^{2SW}, p, \sigma^{1SW}, \sigma^{2SW})$$

2.4. Prior distributions

For the marine survival parameters s^{1SW} and s^{2SW} , we set the same informative priors as **Pardo et al. (2021)**. That is, for the log-transformed at sea survival parameters (the instantaneous mortality rates) $z^a = -\log(s^a)$, $a = 1SW, 2SW$, we set lognormal prior distributions:

$$(10) \quad z^{1SW} \sim \text{lognormal}(1, 0.22)$$

$$(11) \quad z^{2SW} \sim \text{lognormal}(0.2, 0.3)$$

These priors favor such values of the marine survival parameters that **Pardo et al. (2021)** considered to be biologically realistic based on previous studies.

For the proportion of salmon that return to spawn after 1 year at sea, we set

$$(12) \quad \text{logit}(p) \sim \begin{cases} \text{Normal}(2.3, 0.4) & \text{for 1SW-dominated populations} \\ \text{Normal}(0, 2.8) & \text{for non-1SW-dominated populations} \end{cases}$$

For 1SW populations, this prior is concentrated to lower values than the one used by **Pardo et al. (2021)** (Supplementary Material, Figure S1a), while for 2SW populations, our prior is somewhat less informative (Supplementary Material, Figure S1b).

The change-point inference may considerably depend on the amount of random variation that we assume to be present in the empirical time series (**Tirronen et al. 2021**). Thus, the priors of σ^a having been set to

$$(13) \quad \sigma^a \sim \text{half-normal}(\sigma_{\text{reg}}^a, \delta^a), \quad a = 1SW, 2SW$$

we carried out sensitivity analyses in terms of the hyperparameters σ_{reg}^a and δ^a . While this prior does not limit the maximum amount of random variation we assume to be present in the data, the hyperparameter σ_{reg}^a defines the minimum amount of random variation while δ^a controls the relative likelihood of the possible values of σ^a . We first studied the impact of δ^a on the change-point inference by setting $\delta^{1SW} = \delta^{2SW}$ and using the values 0.5, 1, 2, 3, not bounding the amount of random variation from below ($\sigma_{\text{reg}}^a = 0$). Secondly, we tested the sensitivity of change-point inference in terms of σ_{reg}^a with $\delta^{1SW} = \delta^{2SW} = 1$. In this, we set $\sigma_{\text{reg}}^{1SW} = \sigma_{\text{reg}}^{2SW}$, and tested the values 0, 0.02, 0.03, 0.05, 0.1, 0.2 for all data sets

(Supplementary Material, Table S2). For some rivers, we also fitted the model using different values for $\sigma_{\text{reg}}^{1\text{SW}}$ and $\sigma_{\text{reg}}^{2\text{SW}}$, when such a choice was assumed to result in a better fit to the data (Supplementary Material, Table S3). In this, we also used $\delta^a = 0.5$ for some populations.

The conditional prior on the change point was defined using a constant hazard function (Adams and MacKay 2007).

$$(14) \quad p(r_t|r_{t-1}) = \begin{cases} \frac{1}{\lambda} & \text{if } r_t = 0 \\ 1 - \frac{1}{\lambda} & \text{if } r_t = r_{t-1} + 1 \\ 0 & \text{otherwise} \end{cases}$$

for $t = 2, \dots, T$. With this model, the prior probability of a change point is $1/\lambda$. Moreover, we assumed that a change point occurred before the first data point, i.e., $p(r_1 = 0) = 1$, and set a high prior probability of a change point, $\lambda = 5$, which is close to a single generation for salmon. As for the variance parameters, we carried out sensitivity analyses in terms of λ by testing higher values ($\lambda = 10, 20, 30$) with $\sigma_{\text{reg}}^a = 0$ and $\delta^a = 1$ (Supplementary Material, Table S1).

2.5. Change-point detection and parameter inference

We fitted the change-point model to the empirical data by applying the BOCPD method developed by Adams and MacKay (2007), combined with simulation-based filtering (Liu and West 2001; Perälä et al. 2017). The method is sensitive to changes in sequential data and provides a potential tool for detecting temporal changes in the underlying processes that generate ecosystem data. It has been extensively validated for stock–recruitment models (Perälä et al. 2017; Tirronen et al. 2021), and its performance in parameter inference in short segments has also been found decent (Tirronen et al. 2021).

The method processes data in a sequential manner, starting a new run at each time point, updating estimates for the parameter values in the existing runs and computing posterior probabilities of the run lengths (Appendix A). In missing years, the parameter posteriors were assumed not to change but a new run was started to account for the possibility of a change point. In such years, the run length posteriors were computed using one-step predictions (Perälä et al. 2017).

The run length posterior probabilities obtained in filtering were used for computing smoothed run length probabilities (Discussion; Perälä et al. 2017), i.e., run length probabilities in retrospect, given the whole data. The smoothed run length probabilities are not affected by single outliers and were used for dividing the data sets into segments. Following Perälä et al. (2017), we looked for the most likely segmentation (MLS) of each data set by maximizing the product of the smoothed run length probabilities over all possible segmentations (Appendix A). In MLS, we set the maximum number of segments to five and considered only segments that consisted of at least 3 years, except at the beginning and the end of the time series, since the data cannot tell when the first segment started or the last one ended.

In parameter inference, we considered the conditional probability distribution of the model parameters given the data belonging to a given segment at time t (the run-specific

posterior distribution of the model parameters). Particularly, we looked at the posterior distributions at the end of the segments so that all the data in a segment contributed to the inferred parameter values in that segment. In addition to run-specific estimates, the chosen approach provides full parameter posterior distributions which account for the uncertainty related to the timing of the change points.

When combined with simulation-based filtering, BOCPD is a stochastic method. Thus, there was some variation between inferred change points and parameter values when fitting was repeated by using a different set of random samples in the filter, although the priors of the variance parameters σ^a or the change-point prior were not changed. The amount of variation was decreased when the number of samples was increased. The stability of the results also depended on how informative priors were used for the variance parameters. To estimate the robustness of change-point inference with a chosen number of random samples in the filter, we repeated the model fitting twice using different random samples. In this, we used 3×10^6 to 5×10^6 samples in the filter, which resulted in sufficiently low variation in the inferred change points. Moreover, for parameter estimates, we produced a third replicate of the results.

3. Results

3.1. Change points

Using the MLS method, our segmentation analysis detected change points for all rivers except WAB (Table 1; Figs. 2 and 3). For all such rivers except Trinité, the number of inferred change points was dependent on the prior distributions of the variance parameters as well as the change-point prior (Supplementary Material, Tables S1–S3). Evidence of two change points was found for Saint-Jean, while for other rivers with inferred change points the results indicated a single temporal shift in the parameters. However, the data of the studied populations spanned across different time periods. Moreover, with some priors, MLS indicated two shifts in the parameters for Conne but the second change point was not supported by the posterior predictive distributions of 2SW fish, which suggested a better model fit to the data with two segments (Supplementary Material, Figures S10 and S11). Two change points were also inferred for LaHave, but the first segment consisted of 1 year and was found only when the variance parameters were not bound below.

Intriguingly, the results indicated different years of change points for all rivers except two: Saint-Jean and Trinité, in QC. While a change point was inferred for Trinité in 1993, the results suggested a shift in the marine survival parameters for Saint-Jean in 1992 or 1993 (Supplementary Material, Tables S1–S3). However, for one of the analysed populations in NL, Conne, the inferred year of a change point (1991) was close to the timing of the change points for Saint-Jean and Trinité. For the other two populations in NL, the Campbellton time series did not include data before 1994, while for WAB, no change points were inferred, although data were available already in 1974. Neither the LaHave population in NB nor the Nashwaak population in NS had data before 1994. But, the years of

Table 1. The SW dominance of each river studied, the years of change points inferred in the most likely segmentation (MLS), the posterior medians of the Murphy's maturity schedule model parameters in the segments (the time period is shown in parenthesis) using river-specific prior settings for the variance parameters (Supplementary Material, Table S3), and the hazard rate $\lambda = 5$.

River	Posterior medians in MLS				
Name	SW-dominance	Years of change points	s^{1SW}	s^{2SW}	p
Campbellton	1	2005	0.055 (1994–2004)	0.012	0.934
			0.083 (2005–2015)	0.068	0.949
Conne	1	1991	0.089 (1988–1990)	0.201	0.932
			0.036 (1991–2015)*	0.142*	0.939
LaHave	2	2014	0.035 (1997–2013)	0.260	0.614
			0.017 (2014–2017)*	0.223*	0.341*
Nashwaak	2	2013	0.068 (1999–2013)	0.291	0.497
			0.042 (2014–2017)*	0.269*	0.567
Saint-Jean	2	1992, 2009	0.056 (1990–1991)	0.301	0.096
			0.036 (1992–2008)*	0.247*	0.120
			0.060 (2009–2015)	0.291	0.109*
Trinité	2	1993	0.049 (1985–1992)	0.274	0.413
			0.027 (1993–2016)*	0.239*	0.330*
Western Arm Brook (WAB)	1	—	(1974–2015)	—	—

Note: The models were fitted using three different random samples, which resulted in some differences in the estimates (Supplementary Material, Tables S10–S12). The posteriors were estimated using 10^4 samples.

*Indicates a decrease in a posterior median between two consecutive segments.

change points inferred later for LaHave and Nashwaak were close to each other (2014 and 2013, respectively). On the other hand, these two rivers were the only ones having data until 2017, while for almost all other rivers, data were only available until 2015. Nonetheless, the year of change point inferred for Campbellton and also the second change point of Saint-Jean were not close to any other inferred change point.

Naturally, there was some uncertainty included in the change-point detection (Figs. 4 and 5). For Campbellton, both the filtered and smoothed run length probabilities clearly indicated a single temporal change in the marine survival parameters, with some uncertainty, while for Conne, there was more uncertainty included in the posterior run length probabilities. Particularly, between 2000 and 2010, the smoothed run length probabilities indicated the possibility of change points for Conne, although MLS did not include such change points because of their low probability. Despite the differences in the patterns, there could have been approximate synchrony around 2005 between Campbellton and Conne. Moreover, the filtered run length probabilities for WAB indicated the possibility of a change point at the beginning of the 1990s and in 2010, but the smoothed run lengths did not provide evidence for such change points. Among the populations in QC, the smoothed run length probabilities suggested the possibility of a change point around 2000 for both Trinité and Saint-Jean, in addition to the change points at the beginning of 1990s. However, such synchrony between these rivers seemed to have been vanished later. For the NB and NS rivers, there was more uncertainty about a change point at the beginning of the recording period for Nashwaak, than for La-

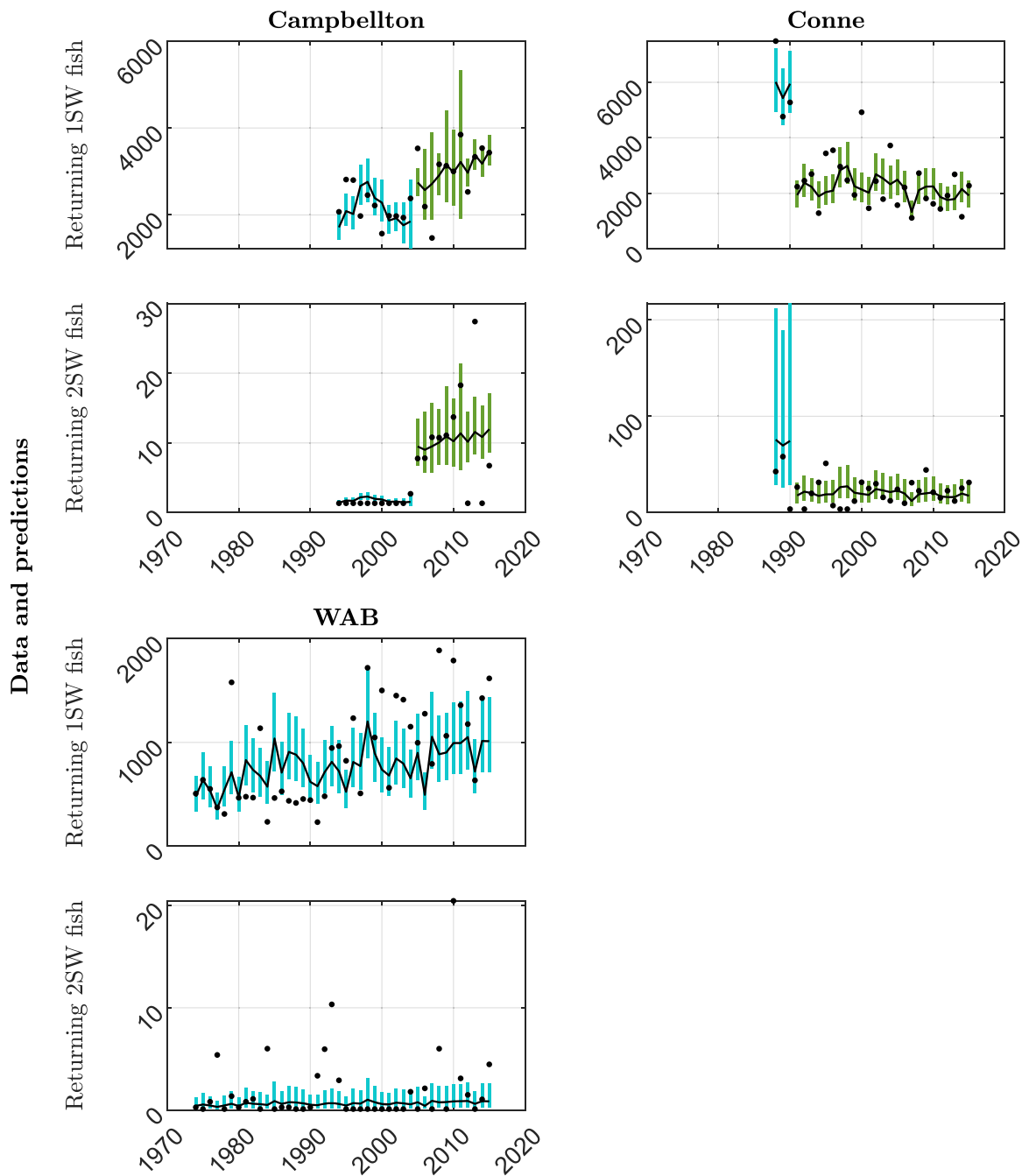
Have. For both of the rivers, the timing of the change point in the 2010s included a considerable amount of uncertainty.

Considering change-point detection, it should be noted, that the approximated measurement errors and the priors set for the variance parameters may have played a considerable role since they together define the total amount of variation around the average values. On average, the measurement error of 2SW fish was high for all 1SW populations (the mean of ϵ^{2SW} was 0.74 for Campbellton, 0.71 for WAB and 0.55 for Conne, while it was <0.08 for all 2SW populations). However, the measurement error of 1SW fish was low for all populations except Campbellton (the mean of ϵ^{1SW} was 0.21 for Campbellton, and <0.07 for other populations). Moreover, a high amount of scatter among successive years in the data can affect parameter inference and consequently, the accuracy of change-point detection (Tirronen et al. 2021). Setting more informative priors for variance parameters may yield to more accurate parameter inference and change-point detection. For some of the studied populations, tighter priors provided more evidence for change points (Supplementary Material, Table S2).

3.2. Parameter estimates

Since the methods we used do not distinguish between changes in the model parameters, all the parameters could contribute to the inferred change points. However, for all rivers except Campbellton, due to the high amount of uncertainty in the estimates of s^{2SW} , the results more clearly indicated shifts in s^{1SW} than in s^{2SW} (Fig. 6; Supplementary

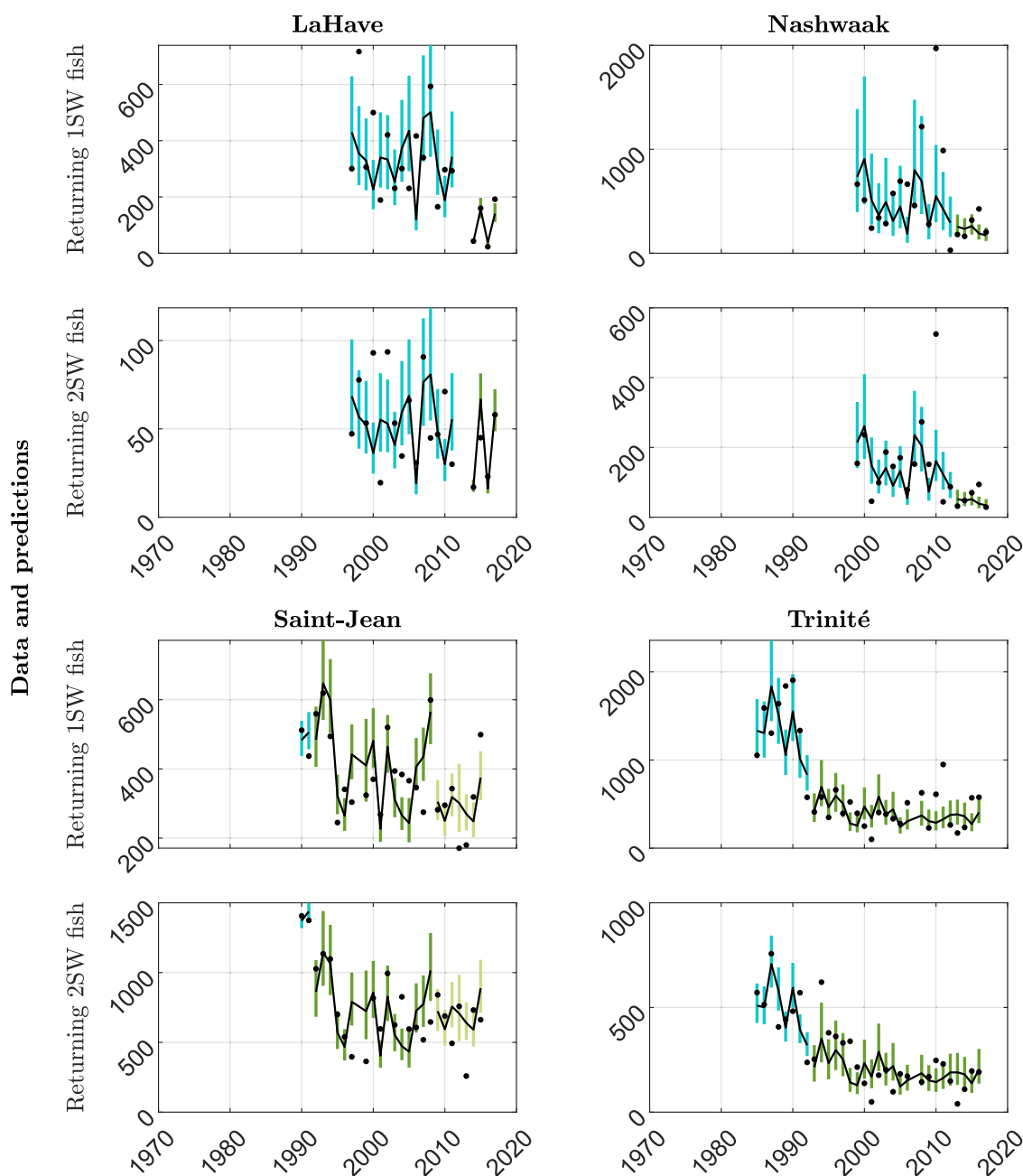
Fig. 2. The analysed time series of the returning 1SW and 2SW fish and the corresponding posterior predictive distributions for the studied populations in NL (Fig. 1). The black solid lines correspond to the medians, while the coloured bars illustrate the intervals between the 0.25th and 0.75th quantiles. The change-point model was fitted to the data sets with the hazard rate $\lambda = 5$, using river-specific prior settings for the variance parameters (Supplementary Material, Table S3).



Material, Figure S7). Also, the estimates of p contained a high amount of uncertainty (Supplementary Material, Figure S6) and, compared to the posteriors of s^{1SW} , shifts in p were more uncertain for all rivers with change points except LaHave (Supplementary Material, Figure S6c). For 2SW populations, the estimates of s^{1SW} also contained rather high amount of uncertainty, reflecting the less informative prior set for p for these populations.

Nonetheless, among the NL populations, the posteriors suggested a steady decline in s^{1SW} for Conne (also when two change points were inferred), increased at-sea survival for Campbellton and no stepwise change for WAB (Fig. 6). For the rivers in QC, both Trinité and Saint-Jean experienced a decline in s^{1SW} at the beginning of the 1990s, but evidence for another temporal change in at-sea survival was only found for Saint-Jean, for which the posteriors suggested a

Fig. 3. The analysed time series of the returning 1SW and 2SW fish and the corresponding posterior predictive distributions for the studied populations in QC, NB, and NS (Fig. 1). The black solid lines correspond to the medians, while the coloured bars illustrate the intervals between the 0.25th and 0.75th quantiles. The change-point model was fitted to the data sets with the hazard rate $\lambda = 5$, using river-specific prior settings for the variance parameters (Supplementary Material, Table S3).

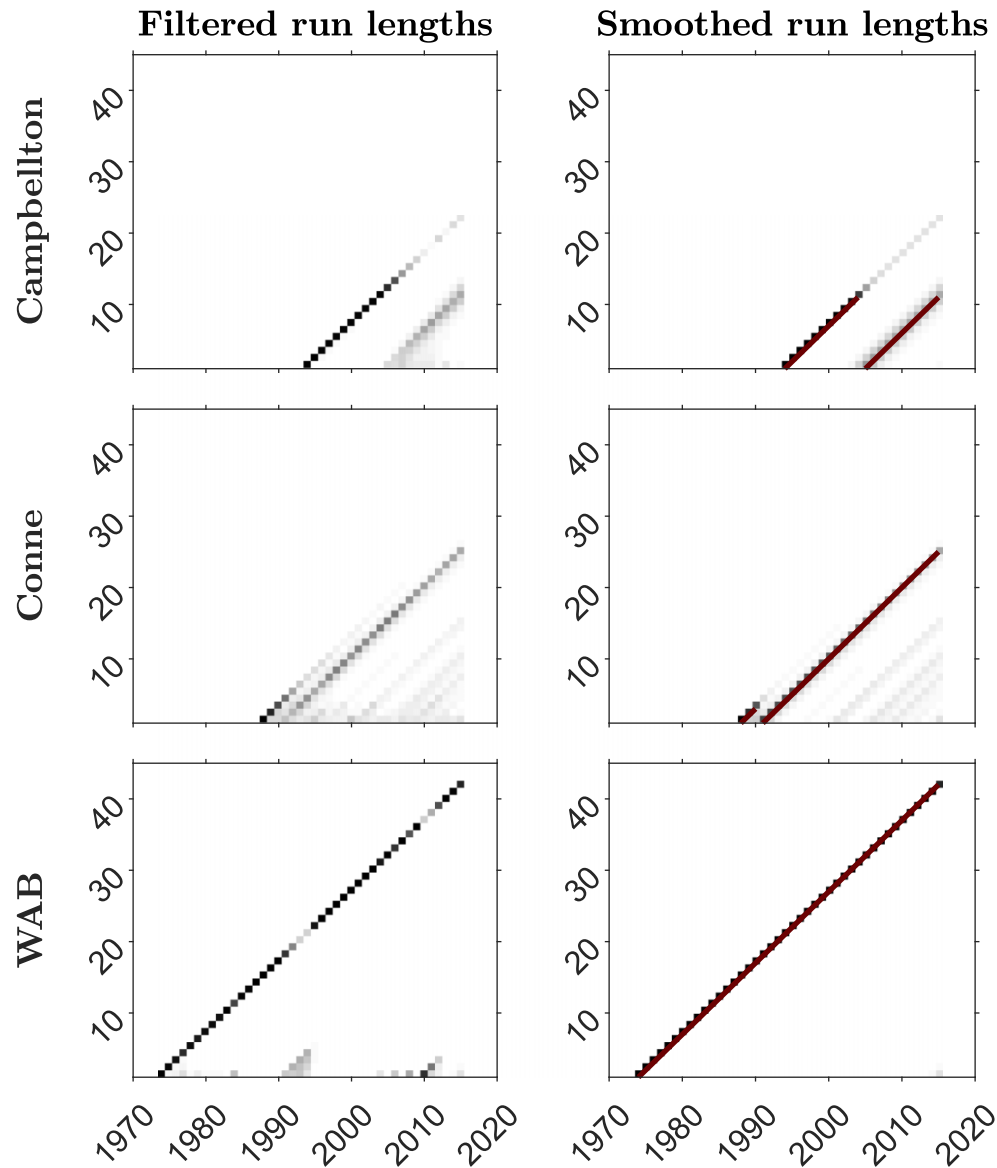


recovery approximately to the same level as s^{1SW} was in the first segment. For Nashwaak (NB) and LaHave (NS), the posteriors suggested a decline in s^{1SW} in 2013–2014. For Campbellton, there was a considerable shift in the number of returning 2SW fish between the segments (no 2SW fish in the first segment except the last year, some 2SW fish in almost every year in the second segment; Fig. 2) and the method also estimated an increase in s^{2SW} . For other rivers with inferred change points, there could be a decrease in s^{2SW} . However, for Saint-Jean, the posteriors suggested that s^{2SW} was decreased

only during the second segment, after which s^{2SW} increased to the same level as it was in the first segment. The estimates of p suggested an increase in p for both NL populations with change points; Campbellton and Conne. Such a change was also suggested for Nashwaak and, during the second segment, for Saint-Jean. A decline in p was suggested for LaHave and Trinité.

The full posterior distributions of s^{1SW} , which take into account the uncertainty of change points, resembled the ones by Pardo et al. (2021) for all rivers (Supplementary Material,

Fig. 4. Posterior run length probabilities after filtering (left) and smoothing (right) for the studied populations in NL (Fig. 1). Black corresponds to a probability of one, white corresponds to a probability of zero. The most likely segmentation is depicted by a red line. The change-point model was fitted to the data sets with the hazard rate $\lambda = 5$, using river-specific prior settings for the variance parameters (Supplementary Material, Table S3).



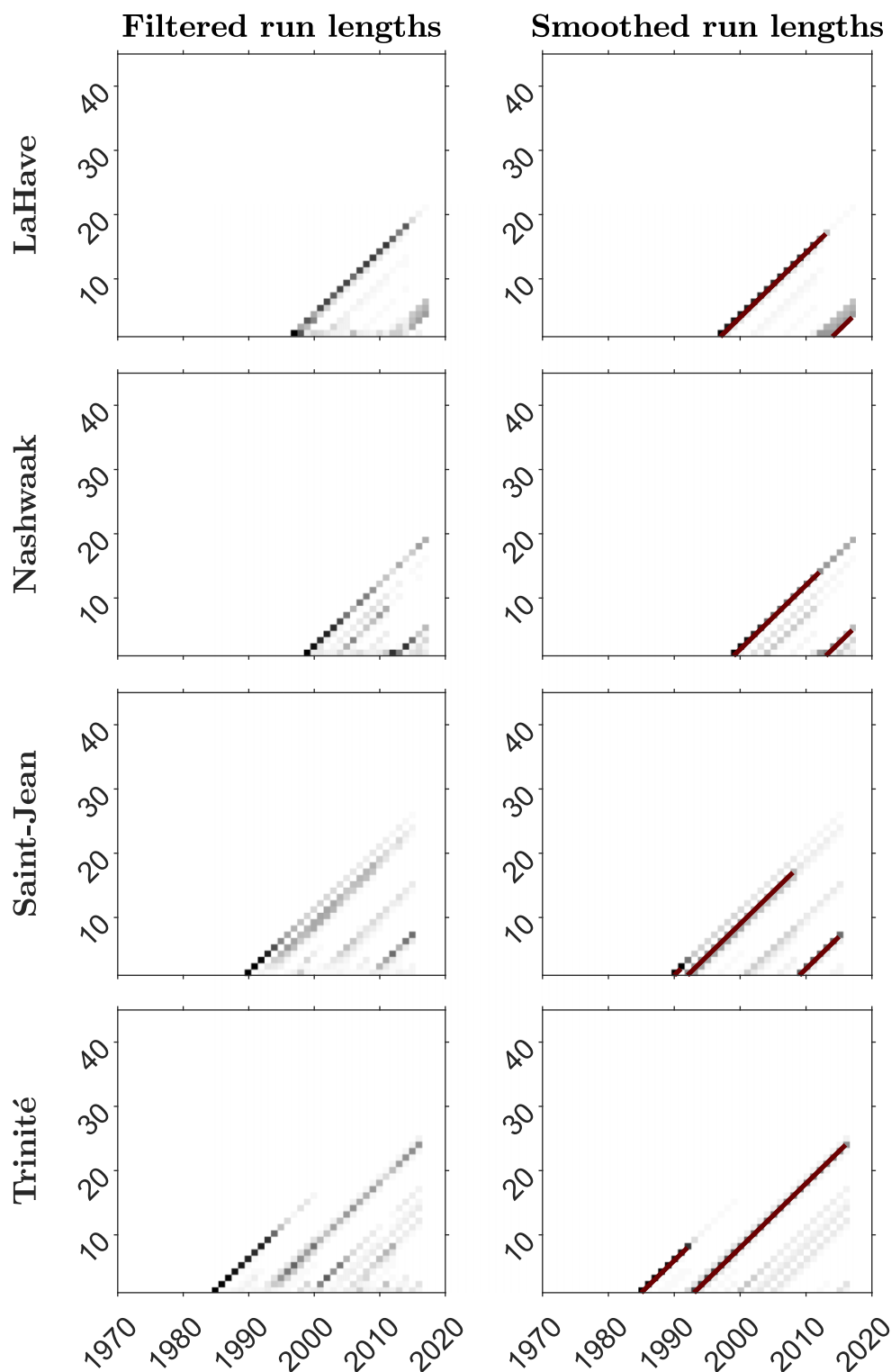
Section S2.1). For 2SW populations, the estimates of s^{2SW} and p also resembled the ones by Pardo et al. (2021) but for 1SW populations, our estimates were lower, reflecting the different prior used for p . Indeed, the posteriors we obtained for p for 1SW populations were concentrated on lower values than the ones obtained by Pardo et al. (2021) and, equivalently, the proportions of fish that stay 2 years at sea ($1 - p$) were estimated higher in our study, yielding to lower s^{2SW} estimates. However, all the differences in the parameter estimates were not due to different prior settings, but the different structure of the model and the accompanying method used for parameter estimation. Particularly, for Campbellton and WAB, successive years of having zero 2SW fish (Fig. 2) did not remarkably impact the estimates of p but produced consider-

ably low estimates for s^{2SW} . For Campbellton, the number of 2SW fish were zero in all years except the last one in the first inferred segment which yielded to extremely low estimates for s^{2SW} in the first segment. Regarding the differences in the posterior distributions, it should also be kept in mind that, as we relied on the estimates of smolt abundances by Pardo et al. (2021), there were some differences in the analysed smolt data between these studies.

4. Discussion

Broad-scale environmental changes have been linked to broad-scale patterns in salmon productivity (Friedland et al. 2003, 2014; Olmos et al. 2019, 2020). Our analyses com-

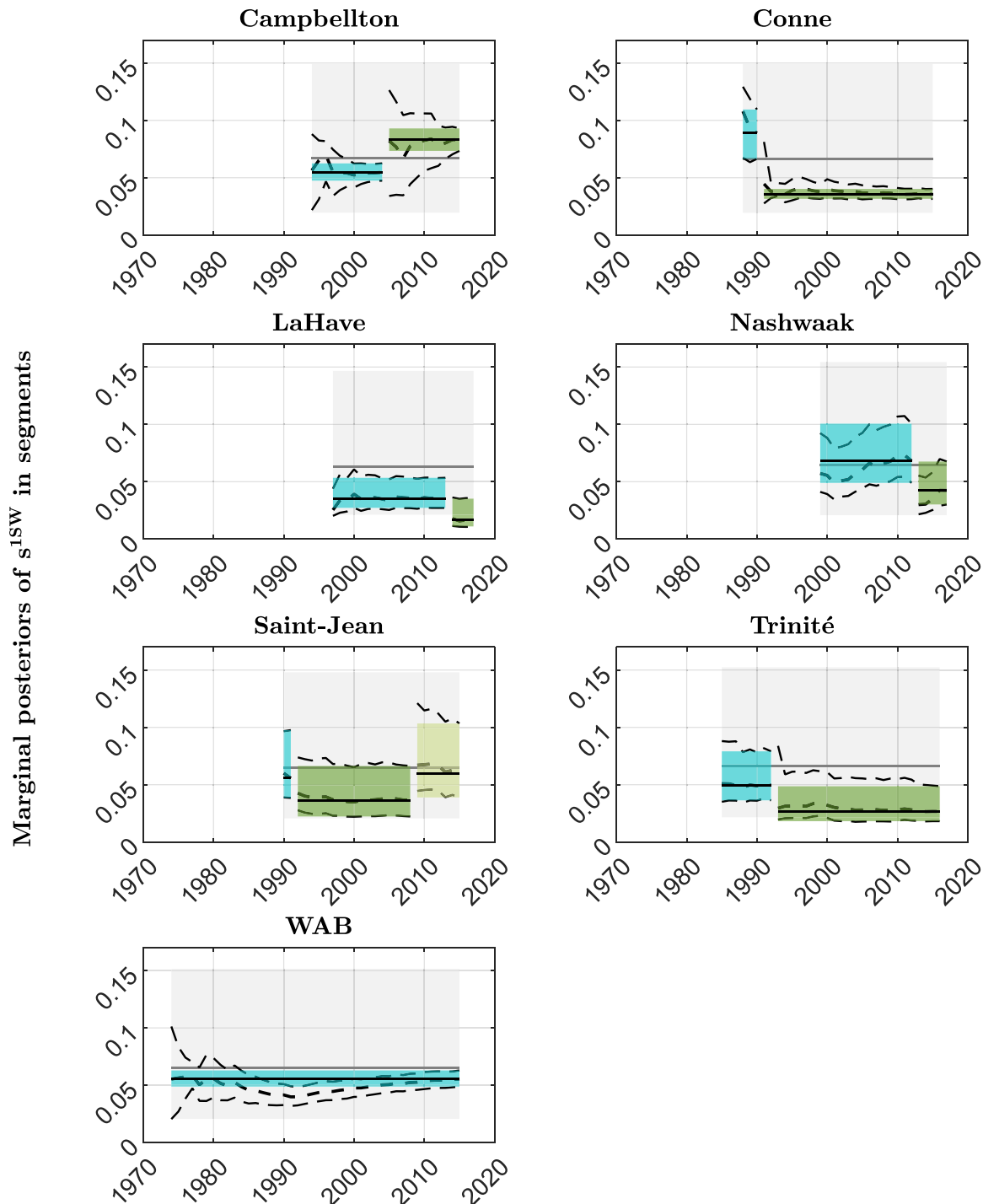
Fig. 5. Posterior run length probabilities after filtering (left) and smoothing (right) for the studied populations in QC, NB, and NS (Fig. 1). Black corresponds to a probability of one, white corresponds to a probability of zero. The most likely segmentation is depicted by a red line. The change-point model was fitted to the data sets with the hazard rate $\lambda = 5$, using river-specific prior settings for the variance parameters (Supplementary Material, Table S3).



plement these efforts by drawing attention to the importance of smaller-scale, possibly population-specific, influences on trends in Atlantic salmon survival (Pardo et al. 2021). Supported by the strongest empirical data on numbers of

outmigrating smolts and returning adults throughout the species' North American range, we have identified different temporal patterns in salmon mortality during the first year at sea. Populations differed in the number of survival

Fig. 6. The marginal posterior distributions (the vertical axes) of the parameter s^{1SW} (the proportion of salmon surviving in their first year at sea) of the Murphy's maturity schedule model with respect to time (the horizontal axes) inferred by the Bayesian online change-point detection method. The shaded areas illustrate the prior distributions (grey) and the posterior distributions according to the most likely segmentation (different colours), the latter ones inferred at the end of the segments. The shaded areas correspond to the intervals between the 0.05th and the 0.95th percentiles while the solid lines correspond to the medians of the posteriors. Similarly, the dashed lines show the 0.05th and 0.95th percentiles of the posterior distributions and their medians after each time step, as inferred by the method. The change-point model was fitted to the data sets with the hazard rate $\lambda = 5$, using river-specific prior settings for the variance parameters (Supplementary Material, Table S3).



change points, the timing of temporal changes, and directional trajectories in mortality. Among four populations for which data extended to at least 1990, Saint-Jean experienced two shifts in s^{1SW} ; first a decline and then a recovery.

Conne and Trinité experienced a single temporal change (a decline), whereas evidence for a change in at-sea survival for WAB was not found during 1974–2015. Among the three populations for which data extended to the mid- or late

1990s, all of them experienced single shifts in s^{1SW} , declining for two (LaHave and Nashwaak) and increasing for one (Campbellton).

Given the widespread, empirically supported assumption that all salmon from North America migrate from their specific coastal areas to the Labrador Sea to feed (Olmos et al. 2020), our work suggests that population differences in survival at sea cannot be fully explained by shared environmental conditions on these feeding grounds. One possibility is that the strength of a shared, survival-based stressor has waned over time, being more important in the early 1990s, when three populations experienced a change point in at-sea survival, than in the subsequent decades. This conclusion would be consistent with the observation that relationships between North Pacific Ocean climate indices (Pacific Decadal Oscillation, North Pacific Gyre Oscillation) and regional physical and ecological processes have weakened over time (Litzow et al. 2020).

It is also likely that interpretative differences in the perceived importance of broad- versus small-scale stressors on salmon survival can be attributed, in part, to differences in data sources. Olmos et al. (2020), for example, reported that post-smolt survival trends for six North American and seven European “stock units” or SUs (ICES 2015, 2017) are synchronous and can be linked with sea surface temperature and primary production. Following ICES (2015, 2017), these SUs represent an amalgamation of data from an undocumented number of populations to estimate salmon survival at large spatial scales (e.g., France, Newfoundland, England and Wales, USA). Rather than relying solely on smolt and returning-adult abundance data, the SU-based estimates of salmon survival depend heavily on catch data, a source with biases that can prove problematic (e.g., Walters 2003). A third potential issue associated with the ICES’s data amalgamation is the inclusion of populations and stock units that are solely sustained by hatcheries (e.g., US populations), a source of potential bias when evaluating patterns of population survival (Fraser 2008; NASCO 2017). Independently of the data sources used to delineate the SUs, temporal synchrony is not a strong element that emerges from our analyses of population-specific data associated with rivers located within four of the six North American SUs.

The importance of small-scale, potentially population-level processes has been previously recognized. Olmos et al. (2019, 2020) noted that despite some broad-scale, spatial coherence in survival trends throughout the north Atlantic, unexplained annual and regional differences remain. Friedland et al. (2014) hypothesized that southern North American populations might be more susceptible to increased predator-related mortality during the post-smolt period than northern populations. A combination of small salmon population sizes (COSEWIC 2011) and increased abundance of highly mobile mammalian predators (predation by grey seals (*Halichoerus grypus*) is related to a lack of recovery in several southern Canadian marine fishes; Swain and Benoit 2015; Neuenhoff et al. 2019) lends credence to this hypothesis. On the other hand, smolt-releases can have an impact on survival, since the releases may buffer predation of wild salmon when they are coming out of the rivers, due to preda-

tor swamping from increased smolt abundance (Furey et al. 2016). Nonetheless, all hatchery fish were excluded from our smolt and adult salmon estimates. It is also instructive to observe that the most considerable declining shift in at-sea survival was found for Conne River, the population with the closest proximity to salmon aquaculture operations, whose negative consequences to wild salmon have been well documented (McGinnity et al. 2003; Sylvester et al. 2019; Bradbury et al. 2020). Potential mechanisms for the lack of synchrony may also include freshwater carryover effects, such as the impact of river acidification on marine survival (Thorstad et al. 2013) which suggest that among-river variability in freshwater conditions, and not just estuarine/coastal differences, could also explain the asynchrony we observed in survival at sea. Furthermore, growth rate at sea is known to correlate with marine survival and can affect probability of returning as 1SW (Friedland et al. 1993). However, of particular importance could be the effect of freshwater growth rate on smolt age and phenology, which then directly impacts marine survival through size-dependent mortality and outmigration mismatch with optimal conditions, respectively (Russell et al. 2012; Jonsson et al. 2017; Gregory et al. 2018). The direct mechanisms behind these relationships (e.g., temporal differences in prey availability, predator avoidance) could be many but little is known about them yet. Freshwater effects not only impact egg-to-smolt survival, which is the life history trait with the highest variability in their life cycle, but also influence what comes after, at sea.

Although we studied marine survival on a smaller scale than Pardo et al. (2021), we recognize that changes may occur in even smaller temporal scale. The model we used describes stepwise changes in the marine survival parameters, ignoring, e.g., continuous linear changes that can also be present in the data (Pardo et al. 2021). Moreover, regarding our results, it should be noted that the change-point prior and the amount of random variation around the average relationship between the number of smolts and returning fish, that was assumed to be present in the data, may have had a considerable impact on change-point inference (Tirronen et al. 2021). Nonetheless, we carried out sensitivity analyses in terms of the priors of the variance parameters as well as the change-point prior, and the obtained posterior predictive distributions suggest that the change points we reported yield a good model fit to the data (Supplementary Material, Section S3). In addition, the priors set for the marine survival parameters may have played a considerable role in parameter estimation. As the focus of this study was on change points, we did not test alternative priors for the survival parameters but, using a different prior for p than that of Pardo et al. (2021), it was evident that the role of such priors can be considerable. Furthermore, with the priors we chose to use, we could not infer temporal changes in s^{2SW} or p , since the posterior distributions of these parameters contained a large amount of uncertainty. In the previous study (Pardo et al. 2021), the estimates obtained for s^{2SW} and p were also highly uncertain.

The present study suggests that a critical component in Atlantic salmon life history, survival during the first sea win-

ter, depends nontrivially on local or regional conditions. Our findings are not consistent with the hypothesis that salmon populations consistently share the same mortality-related stressors in the marine environment. Although populations may have shared greater synchrony in survival patterns in the past, this synchrony may be breaking down, as reflected by a lack of temporal concordance in survival change points. Rather than focus primarily on putative large-scale stressors, it may be prudent to direct greater attention to smaller-scale regional or population-level correlates of survival. This is further supported by genomic data on the fine-scale metapopulation structuring and source–sink dynamics among nearby salmon rivers (Hindar et al. 2004; Kuparinen et al. 2010) as well as genetic and life history differentiation within salmon river tributaries (e.g., Vähä et al. 2007). Although challenging, the technology for population identification based on genomic markers does exist (Vähä et al. 2016; Bernatchez et al. 2017). From the perspective of environmental management, a focal shift from broad-scale oceanographic patterns to smaller-scale regional or local conditions implies a need to consider interactions among terrestrial and aquatic systems as well as human impacts on aquatic habitats. While the present study takes a step towards understanding the timing and scale of drivers affecting salmon survival in the sea, little is still known about the underlying mechanisms and the response times, particularly, how and when conditions experienced at egg, larval, and juveniles stages affect salmon later in its life.

Acknowledgements

We thank Yong Chen and two anonymous reviewers who provided many helpful suggestions, which significantly improved the manuscript. The present study reflects only the authors' view; the European Research Council is not responsible for any use that may be made of the information it contains.

Article information

History dates

Received: 5 November 2021

Accepted: 22 April 2022

Accepted manuscript online: 20 May 2022

Version of record online: 27 September 2022

Copyright

© 2022 The Author(s). This work is licensed under a [Creative Commons Attribution 4.0 International License](https://creativecommons.org/licenses/by/4.0/) (CC BY 4.0), which permits unrestricted use, distribution, and reproduction in any medium, provided the original author(s) and source are credited.

Data availability

All data that support the plots and other findings in this paper are available from the corresponding author upon reasonable request. Source data and code are available at <https://doi.org/10.5061/dryad.9p8cz8wjg>.

Author information

Author ORCIDs

Maria Tirronen <https://orcid.org/0000-0001-6052-3186>

Author notes

Jeffrey A. Hutchings is deceased.

Author contributions

MT was responsible for formal analysis, methodology, software, visualization, writing — original draft, writing — review and editing. JAH was responsible for conceptualization, funding acquisition, writing — original draft. SAP was responsible for conceptualization, methodology, writing — review and editing. AK was responsible for funding acquisition, supervision, writing — original draft, writing — review and editing.

Competing interests

The authors declare there are no competing interests.

Funding information

This work was funded by the Atlantic Salmon Conservation Foundation and by the Academy of Finland (project grant 317495 to AK), Natural Sciences and Engineering Research Council of Canada (NSERC; Discovery Grants to JAH and AK), and the European Research Council (COMPLEX-FISH 770884 to AK).

Supplementary material

Supplementary data are available with the article at <https://doi.org/10.1139/cjfas-2021-0302>.

References

- Adams, R.P., and MacKay, D.J.C. 2007. Bayesian online changepoint detection. Technical report. Available from <https://arxiv.org/abs/0710.3742>.
- Bernatchez, L., Wellenreuther, M., Araneda, C., Ashton, D., Barth, J., Beacham, T., et al. 2017. Harnessing the power of genomics to secure the future of seafood. *Trends Ecol. Evol.* **32**:665–680. doi:10.1016/j.tree.2017.06.010.
- Bradbury, I., Duffy, S., Lehnert, S.J., Jóhannsson, R., Fridriksson, J.H., Castellani, M., et al. 2020. Model-based evaluation of the genetic impacts of farm-escaped Atlantic salmon on wild populations. *Aquac. Environ. Interact.* **12**: 45–59. doi: 10.3354/aei00346.
- COSEWIC. 2011. COSEWIC assessment and status report on Atlantic salmon *Salmo salar* in Canada. Committee on the Status of Endangered Wildlife in Canada, Ottawa, Canada. Available from https://wildlife-species.canada.ca/species-risk-registry/virtual_sara/files/cosewic/sr_Atlantic_Salmon_2011a_e.pdf.
- Fraser, D. 2008. How well can captive breeding programs conserve biodiversity? A review of salmonids. *Evol. Appl.* **1**: 535–586. doi:10.1111/j.1752-4571.2008.00036.x.
- Friedland, K.D., Reddin, D.G., and Kocik, J.F. 1993. Marine survival of North American and European Atlantic salmon: effects of growth and environment. *ICES J. Mar. Sci.* **50**: 481–492. doi:10.1006/jmsc.1993.1051.
- Friedland, K.D., Reddin, D.G., and Castonguay, M. 2003. Ocean thermal conditions in the post-smolt nursery of North American Atlantic salmon. *ICES J. Mar. Sci.* **60**: 343–355. doi:10.1016/S1054-3139(03)00022-5.
- Friedland, K.D., Shank, B.V., Todd, C.D., McGinnity, P., and Nye, J.A. 2014. Differential response of continental stock complexes of At-

- lantic salmon (*Salmo salar*) to the Atlantic Multidecadal Oscillation. *J. Mar. Syst.* **133**: 77–87. doi: [10.1016/j.jmarsys.2013.03.003](https://doi.org/10.1016/j.jmarsys.2013.03.003).
- Furey, N., Hinch, S., Bass, A., Middleton, C., Minke-Martin, V., and Lotto, A. 2016. Predator swamping reduces predation risk during nocturnal migration of juvenile salmon in a high-mortality landscape. *J. Anim. Ecol.* **85**: 948–959. doi: [10.1111/1365-2656.12528](https://doi.org/10.1111/1365-2656.12528).
- Gregory, S., Armstrong, J., and Britton, R. 2018. Is bigger really better? Towards improved models for testing how Atlantic salmon *Salmo salar* smolt size affects marine survival. *J. Fish. Biol.* **92**: 579–592. doi: [10.1111/jfb.13550](https://doi.org/10.1111/jfb.13550).
- Hindar, K., Tufto, J., Sættem, L.M., and Balstad, T. 2004. Conservation of genetic variation in harvested salmon populations. *ICES J. Mar. Sci.* **61**(8): 1389–1397. doi: [10.1016/j.icesjms.2004.08.011](https://doi.org/10.1016/j.icesjms.2004.08.011).
- ICES. 2015. Report of the Working Group on North Atlantic Salmon (WGNAS), 17–26 March. ICES CM 2015/ACOM:09. Moncton, Canada. Available from https://www.ices.dk/sites/pub/Publication%20Reports/Expert%20Group%20Report/acom/2015/WGNAS/wgnas_2015.pdf.
- ICES. 2017. Report of the Working Group on North Atlantic Salmon (WGNAS). ICES CM 2017/ACOM: 20. Copenhagen, Denmark. Available from https://www.ices.dk/sites/pub/Publication%20Reports/Expert%20Group%20Report/acom/2017/WGNAS/wgnas_2017.pdf.
- ICES. 2021. Working Group on North Atlantic Salmon. ICES Scientific Reports, Vol. 3. doi: [10.17895/ices.pub.7923](https://doi.org/10.17895/ices.pub.7923).
- Jonsson, B., Jonsson, M., and Jonsson, N. 2017. Influences of migration phenology on survival are size dependent in juvenile Atlantic salmon (*Salmo salar*). *Can. J. Zool.* **95**: 581–587. doi: [10.1139/cjz-2016-0136](https://doi.org/10.1139/cjz-2016-0136).
- Kuparinen, A., Tufto, J., Consuegra, S., Hindar, K., Merilä, J., and Garcia de Leaniz, C. 2010. Effective size of an Atlantic salmon (*Salmo salar* L.) metapopulation in northern Spain. *Conserv. Genet.* **11**: 1559–1565. doi: [10.1007/s10592-009-9945-6](https://doi.org/10.1007/s10592-009-9945-6).
- Litzow, M., Hunsicker, M., Bond, N., Burke, B., Cunningham, C., Gosselin, J., et al. 2020. The changing physical and ecological meanings of north Pacific Ocean climate indices. *Proc. Natl. Acad. Sci. U.S.A.* **117**: 7665–7671. doi: [10.1073/pnas.1921266117](https://doi.org/10.1073/pnas.1921266117).
- Liu, J., and West, M.A. 2001. Combined parameter and state estimation in simulation-based filtering. In *Sequential Monte Carlo methods in practice*. Edited by A. Doucet and N. de Freitas. Statistics for Engineering and Information Science. pp. 197–223.
- Massiot-Granier, F., Prevost, E., Chaput, G., Potter, T., Smith, G., White, J., et al. 2014. Embedding stock assessment within an integrated hierarchical Bayesian life cycle modelling framework: an application to Atlantic salmon in the northeast Atlantic. *ICES J. Mar. Sci.* **71**(7): 1653–1670. doi: [10.1093/icesjms/fst240](https://doi.org/10.1093/icesjms/fst240).
- McGinnity, P., Prodöhl, P., Ferguson, A., Hynes, R., Maoiléidigh, N.O., Baker, N., et al. 2003. Fitness reduction and potential extinction of wild populations of Atlantic salmon, *Salmo salar*, as a result of interactions with escaped farm salmon. *Proc. R. Soc. B*, **270**(1532): 2443–2450. doi: [10.1098/rspb.2003.2520](https://doi.org/10.1098/rspb.2003.2520).
- Murphy, G.I. 1952. An analysis of silver salmon counts at Bendow Dam, South Fork of Eel River, California. *Calif. Fish Game*, **38**: 105–112.
- NASCO. 2017. Understanding the risks and benefits of hatchery and stocking activities to wild Atlantic salmon populations. North Atlantic Salmon Conservation Organization Council Document CNL(17)61. Available from <https://nasco.int/wp-content/uploads/2020/02/2017ThemeBasedSession.pdf>.
- Neuenhoff, R., Swain, D., Cox, S., McAllister, M., Trites, A., Walters, C., and Hammill, M. 2019. Continued decline of a collapsed population of Atlantic cod (*Gadus morhua*) due to predation-driven Allee effects. *Can. J. Fish. Aquat. Sci.* **76**(1):168–184. doi: [10.1139/cjfas-2017-0190](https://doi.org/10.1139/cjfas-2017-0190).
- Olmos, M., Massiot-Granier, F., Prévost, E., Chaput, G., Bradbury, I.R., Nevoux, M., and Rivot, E. 2019. Evidence for spatial coherence in time trends of marine life history traits of Atlantic salmon in the North Atlantic. *Fish. Fish.* **20**(2): 322–342. doi: [10.1111/faf.12345](https://doi.org/10.1111/faf.12345).
- Olmos, M., Payne, M.R., Nevoux, M., Prévost, E., Chaput, G., Du Pontavice, H., et al. 2020. Spatial synchrony in the response of a long range migratory species (*Salmo salar*) to climate change in the North Atlantic Ocean. *Glob. Change Biol.* **26**(3): 1319–1337. doi: [10.1111/gcb.14913](https://doi.org/10.1111/gcb.14913).
- Pardo, S.A., Bolstad, G.H., Dempson, J.B., April, J., Jones, R.A., Raab, D., and Hutchings, J.A. 2021. Trends in marine survival of Atlantic salmon populations in eastern Canada. *ICES J. Mar. Sci.* **78**: 2460–2473. doi: [10.1093/icesjms/fsab118](https://doi.org/10.1093/icesjms/fsab118).
- Perälä, T., Olsen, E., and Hutchings, J. 2020. Disentangling conditional effects of multiple regime shifts on Atlantic cod productivity. *PLoS ONE*, **15**(11):e0237414. doi: [10.1371/journal.pone.0237414](https://doi.org/10.1371/journal.pone.0237414).
- Perälä, T.A., Swain, D.P., and Kuparinen, A. 2017. Examining nonstationarity in the recruitment dynamics of fishes using Bayesian change point analysis. *Can. J. Fish. Aquat. Sci.* **74**(5): 751–765. doi: [10.1139/cjfas-2016-0177](https://doi.org/10.1139/cjfas-2016-0177).
- Russell, I.C., Aprahamian, M.W., Barry, J., Davidson, I.C., Fiske, P., Ibbotson, A.T., et al. 2012. The influence of the freshwater environment and the biological characteristics of Atlantic salmon smolts on their subsequent marine survival. *ICES J. Mar. Sci.* **69**: 1563–1573. doi: [10.1093/icesjms/fsr208](https://doi.org/10.1093/icesjms/fsr208).
- Särkkä, S. 2013. Bayesian filtering and smoothing. Institute of Mathematical Statistics Textbooks, Cambridge University Press. doi: [10.1017/CBO9781139344203](https://doi.org/10.1017/CBO9781139344203).
- Schindler, D., Hilborn, R., Chasco, B., Boatright, C., Quinn, T., Rogers, L., and Webster, M. 2010. Population diversity and the portfolio effect in an exploited species. *Nature*, **465**: 609–12. doi: [10.1038/nature09060](https://doi.org/10.1038/nature09060).
- Scientific Council for Salmon Management. 2019. Status of wild Atlantic salmon in Norway in 2019. Report from the Scientific Council for Salmon Management, No. 12. Full report is available from (in Norwegian) <http://hdl.handle.net/11250/2619889>. English summary is available from <https://www.vitenskapsradet.no/Portals/vitenskapsradet/Pdf/Status%20of%20wild%20Atlantic%20salmon%20in%20Norway.pdf>.
- Swain, D., and Benoît, H. 2015. Extreme increases in natural mortality prevent recovery of collapsed fish populations in a Northwest Atlantic ecosystem. *Mar. Ecol. Prog. Ser.* **519**: 165–182. doi: [10.3354/meps11012](https://doi.org/10.3354/meps11012).
- Sylvester, E.V.A., Wringe, B.F., Duffy, S.J., Hamilton, L.C., Fleming, I.A., Castellani, M., et al. 2019. Estimating the relative fitness of escaped farmed salmon offspring in the wild and modelling the consequences of invasion for wild populations. *Evol. Appl.* **12**(4): 705–717. doi: [10.1111/eva.12746](https://doi.org/10.1111/eva.12746).
- Thorstad, E.B., Uglem, I., Finstad, B., Kroglund, F., Einarssdóttir, I.E., Kristensen, T., et al. 2013. Reduced marine survival of hatchery-reared Atlantic salmon post-smolts exposed to aluminium and moderate acidification in freshwater. *Estuar. Coast. Shelf Sci.* **124**: 34–43.
- Tirronen, M., Perälä, T., and Kuparinen, A. 2021. Temporary Allee effects among nonstationary recruitment dynamics in depleted gadid and flatfish populations. *Fish. Fish.* **23**(2):392–406. doi: [10.1111/faf.12623](https://doi.org/10.1111/faf.12623).
- Vähä, J.-P., Erkinaro, J., Falkegård, M., Orell, P., and Niemelä, E. 2016. Genetic stock identification of Atlantic salmon and its evaluation in a large population complex. *Can. J. Fish. Aquat. Sci.* **74**. doi: [10.1139/cjfas-2015-0606](https://doi.org/10.1139/cjfas-2015-0606).
- Vähä, J.-P., Erkinaro, J., Niemelä, E., and Primmer, C. 2007. Life-history and habitat features influence the within-river genetic structure of Atlantic salmon. *Mol. Ecol.* **16**: 2638–2654. doi: [10.1111/j.1365-294X.2007.03329.x](https://doi.org/10.1111/j.1365-294X.2007.03329.x).
- Walters, C.J. 2003. Folly and fantasy in the analysis of spatial catch data. *Can. J. Fish. Aquat. Sci.* **60**(12): 1433–1436. doi: [10.1139/f03-152](https://doi.org/10.1139/f03-152).
- WWF. 2001. The status of wild Atlantic salmon: a river by river assessment. World Wildlife Fund. Available from https://wwf.panda.org/wwf_news/?3729/The-Status-of-Wild-Atlantic-Salmon-A-River-by-River-Assessment.

Appendix A

Given an underlying predictive model and a change-point prior, the BOCPD method (Adams and MacKay 2007) infers the time since the last change point, the run length, at each time step. For the change-point model with input–output data, the run length posterior distribution can be formulated as (Perälä et al. 2017):

$$(A1) \quad p(r_t | \mathbf{R}_{1:t}, S_{1:t}) \\ = \sum_{r_{t-1}=0}^{t-2} \frac{p(r_t | r_{t-1}) p(\mathbf{R}_t | \mathbf{R}_{t-1}^{(r)}, S_{t-1}^{(r)}, S_t)}{p(\mathbf{R}_t | \mathbf{R}_{1:t-1}, S_{1:t-1}, S_t)}$$

Above, $\mathbf{R}_{t:u} = (\mathbf{R}_t, \dots, \mathbf{R}_u)$ and $\mathbf{R}_u^{(r)} = \mathbf{R}_{(u-r_u):u}$, and similarly, $S_{t:u} = (S_t, \dots, S_u)$ and $S_u^{(r)} = S_{(u-r_u):u}$.

With nonlinear models and arbitrary prior distributions of the model parameters, the posterior distributions of the model parameters are analytically intractable but can be inferred by a sequential Monte Carlo method using artificial evolution of parameters (a particle filter; Perälä et al. 2017; Liu and West 2001). In this, the acceptable number of effective particles was set to half of the number of particles used in the filter. For the smoothing parameter in the particle filter we set the value 0.1, suggested by Liu and West (2001).

A segmentation is a sequence $s = (s_1, \dots, s_T)$ of run lengths for time steps $t = 1, \dots, T$. The MLS of a time series was found

by maximizing the product of the smoothed run length probabilities over all possible segmentations:

$$(A2) \quad \arg \max_s \prod_{i=1}^T p(r_i = s_i \mid \mathbf{R}_{1:T}, S_{1:T})$$

In this, the smoothed run length probabilities were computed recursively using the following equations (Särkkä 2013; Perälä et al. 2017):

$$(A3) \quad p(r_\tau \mid \mathbf{R}_{1:T}, S_{1:T}) = p(r_\tau \mid \mathbf{R}_{1:\tau}, S_{1:\tau}) \sum_{r_{\tau+1}=0}^{\tau} \frac{p(r_{\tau+1} \mid r_\tau) p(r_{\tau+1} \mid \mathbf{R}_{1:T}, S_{1:T})}{p(r_{\tau+1} \mid \mathbf{R}_{1:\tau}, S_{1:\tau})}$$

$$(A4) \quad p(r_{\tau+1} \mid \mathbf{R}_{1:\tau}, S_{1:\tau}) = \sum_{r_\tau=0}^{\tau-1} p(r_{\tau+1} \mid r_\tau) p(r_\tau \mid \mathbf{R}_{1:\tau}, S_{1:\tau})$$